

Article

Practical Method to Evaluate the Effects of the Sensor and the Environment on the Measurement of Lightning-Generated Electric Field Signatures

Albeiro Santa-Acosta^{1,a}, Lina María Morales-García^{1,b},
and Herbert Enrique Rojas-Cubides^{1,2,c,*}

¹ Electrical Systems and Energy Efficiency Research Group (GISE3-UD), Universidad Distrital Francisco José de Caldas, Bogotá, Colombia

² Department of Electrical Engineering, Faculty of Engineering, Universidad Distrital Francisco José de Caldas, Bogotá, Colombia

E-mail: ^aasantaa@correo.udistrital.edu.co, ^blimmoralesg@correo.udistrital.edu.co,

^{c,*}herojasc@udistrital.edu.co (Corresponding author)

Abstract. Indirect lightning measurement, using sensors and remote systems that record the radiated electric fields, is one of the most used methods to study and characterize this type of electrical discharges. This is due to its simplicity of implementation, low cost and the valuable information it provides. However, the measurement of the lightning-generated electric fields (LEF) can be influenced by factors such as the type of sensor, its physical features and its location, as well as by characteristics of the electromagnetic environment like geographical features, the structures that surround the measurement station and the materials of these objects. Under this consideration, this paper proposes a generalized method focused on the identification of those parameters that affect significantly influence the LEF measurement, as well as the process to estimate the correction factor of any measuring system designed for this purpose. This factor is important, as it indicates the proportion in which the signals of interest are attenuated or amplified. The method includes a review about the characteristics of the sensors, their connection scheme and a detailed analysis of the effect of the surrounding structures, taking into account parameters such as the permittivity and electrical conductivity of the materials. Finally, with the aim of presenting quantitative results, the proposed method is validated using as a practical case the information from the LEF automated measuring station owned by the Universidad Distrital Francisco José de Caldas located in Bogotá, Colombia.

Keywords: Correction factor, electric field, electromagnetic environment, electric permittivity, lightning flash, structures.

ENGINEERING JOURNAL Volume 25 Issue 8

Received 2 June 2021

Accepted 10 August 2021

Published 31 August 2021

Online at <https://engj.org/>

DOI:10.4186/ej.2021.25.8.137

1. Introduction

Currently, atmospheric discharges (lightning flashes) are considered as one of the most dangerous natural phenomena around the world. These discharges can cause forest fires, damage to structures, interference in different electronics and telecommunications systems, damage to electrical power systems, and in some cases, it can cause injury or death to people and animals [1]. This last aspect, a fundamental pillar on which the protection against lightning is focused, can cause accidents by direct contact between the individual and the lightning, or indirectly, by the induced currents that produce the rise in electrical potential between one or more contact points.

In general, there are four types of lightning flashes: cloud-atmosphere (CA), cloud-to-cloud (CC), intracloud (IC) and cloud-to-ground (CG). The latter have been the most studied phenomena because they cause the greatest number of harmful effects on people, facilities, structures and equipment. One of the most common techniques to obtain several parameters of CG lightning flashes (magnitude of current, current derivative, polarity, multiplicity, total flash duration, among others) is based on the measurement of the electric and magnetic fields produced during the occurrence of the discharge. From these measurements, it has been possible to establish some predominant characteristics of CG flashes, the study of CC or IC flashes has been conducted, criteria for protection against lightning have been defined and warning networks and lightning location systems have been improved [2]–[6].

In the Colombian case, during the last 15 years, a considerable percentage of studies about lightning flashes have been carried out using indirect measuring systems. In this context, the study of return strokes (RS) of CG flashes has been possible analyzing magnetic field measurements [7]–[9], while electric field waveforms have been used to advance in the characterization of negative CG lightning flashes [9]–[13], positive CG flashes [14] and the preliminary discharges that precede the first return stroke (FRS) [15], [16]. However, a major part of these works, and others published in several countries, have shown that lightning-generated electric fields (LEF) measurements in urban areas are particularly affected by the location of the sensors (ground-surface or a specific height) and the presence of structures or obstacles near to the field point (location where LEF are measured) [9], [17]–[23]. Some of these structures may be natural such as mountains, mountain ranges and trees, while others are created by man such as buildings, houses, metal towers, among others.

From these experiences, it is possible to affirm that any system used to measure LEF is directly influenced by the physical and electromagnetic environment. Likewise, the effects that can be caused by the shape and location of the sensor (antenna), together with the characteristics (physical and electrical) of nearby structures, are different in each case. Therefore, this type of measuring system requires the estimation of an antenna enhancement factor,

also called correction factor by location (CFL). This factor allows adjusting (correct) the measurements and the recorded waveforms and thus having reliable information to carry out lightning studies.

Generalized methods to estimate the effect of tall metallic structures and buildings on the electric/magnetic field measurements are based on theoretical and computer models. Major part of these methods, include lightning return stroke models and the solution of integral equations (Maxwell's equations) in time-domain [17]–[20], the application of the method of moments [22] and static-field estimations [24]. Among the disadvantages of these alternatives are: (a) the computation times; (b) the rough geometric approximation of the structure (wire grid or solid parallelepiped); (c) the materials that can be used (metal or conducting reinforcement); (d) simplification of simulations. In many of these methods, only the structure and the field point are included ruling out the electromagnetic environment and the influence that other structures located in the vicinity of the measuring system may produce.

On the other hand, a practical method to obtain the CFL consists of the simultaneous measurement of electric fields using two antennas with similar characteristics, which are separated by a short distance from the horizontal axis (less than 8 meters in south direction) [21], [22]. In this case, one of the antennas is located at ground level and the other is located in the place where the measuring system will be operating (roof, terrace, mast, stand, etc.). In this way, by simultaneously recording of the LEF signals, it is possible to determine the ratio between the waveforms captured by the antennas (attenuation or amplification). However, this method requires is not entirely reliable since the total absence of obstacles in the vicinity of the antenna located at ground level must be guaranteed, and this, in general, is not possible.

Another method to obtain the CFL is based on 3D simulations that combine electromagnetic software, detailed physical models and numerical methods (finite elements, solvers for integral equations, among others). In this way, some works have been presented in recent years focused on specifically analyzing the influence of the place where the measuring system is installed [10], [13], [23]. However, none of these works present an articulated set of procedures that facilitate the characterization of any LEF measuring system, and at the same time, guide on the selection of materials, the configuration of simulation scenarios, the collection of complementary data. and the estimation of the corresponding CFL.

In this context, this paper proposes a general method to evaluate the influence of sensors, nearby structures and other objects in the measurement of LEF signals. The above includes a review of the characteristics that the sensors must have, the way in which the structures must be configured, the effect of some parameters such as the electrical permittivity of the materials and the influence of the grounding system in the calculation of the CFL. Finally, with the aim of applying and validating the proposed method, a study case is presented using the information

from the indirect lightning measuring station of the GISE3-UD research group, which is installed in Bogotá, Colombia.

2. Electric Field Measuring System

In general terms, an LEF measuring system is composed of five elements: a sensor or antenna, an electronic circuit, a signal acquisition/recording equipment and two coaxial cables to guarantee a suitable coupling between the first three components. A general diagram of this system is shown in Fig. 1. The characteristics of each of the components are briefly described below.

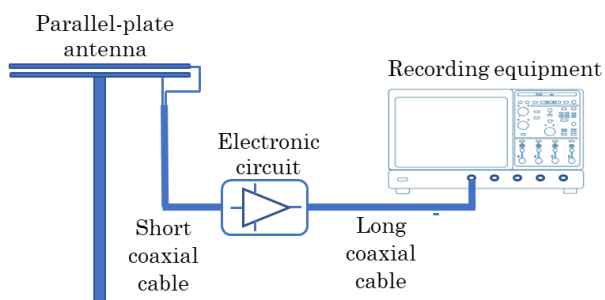


Fig. 1. LEF measuring system.

- Electric field sensor: used to measure the vertical and/or horizontal component of the electric field. In general, an aluminum parallel-plate antenna with circular shape (discs) is used, a 0.03 m of separation between them and a support mast with a physical height between 1.0 and 1.5 meters.
- Short coaxial cable: with 0.6 m long, it is used for the connection between the antenna and the electronic circuit. Often RG-58 A/U coaxial cables with a surge impedance of 50 Ω are used.
- Electronic circuit: based on a high-speed buffer, its function is to provide enough power for the signal captured by the antenna to travel through the long coaxial cable and reach the recording equipment without significant losses.
- Long coaxial cable: with 12 m long, it is used to connect the electronic circuit (located near to the antenna) with the recording equipment.
- Recording equipment: used to register and save the LEF signatures, it can be a transient recorder, a digital acquisition hardware or a digital oscilloscope. It must have sufficient capabilities to capture and save signals with front times of a few microseconds (sampling times between 10 ns and 1 μ s).

It is important to mention that the mast, the bottom plate of the antenna and the outer conductor of the coaxial cables are referenced to the same point, which, as far as possible, should be the grounding system of the place where the measuring system is installed. On the other hand, in the case of the electronic circuit, there are several alternatives (configurations) depending on the buffer-

amplifier used, although the configuration of the circuit is similar in all cases. Although the detailed description of this circuit, as well as its construction and calibration process, are not part of the scope of this work, it is recommended to review the technical features and the methodology described in [13], [25].

Finally, it should be taken into account that, due to space restrictions, the presence of elevated structures around the measuring system, and in some cases, in order to ensure the safety of the equipment, the antenna is usually located in the upper part of a building or structure (roof, terrace or similar). Under this situation, as already mentioned, the estimation of the CFL is even more relevant.

3. Practical Method for Estimating the CFL

As a first aspect, it is important to emphasize that, for measuring systems installed in open-air at ground level without the presence of structures, it is not necessary to estimate the influence of the environment on the measurements. In this case, only the enhancement factor related to the physical height of the antenna and the electronic circuit should be estimated [25]. In this case, the LEF signals will not be affected by the presence of obstacles, nor by abrupt changes in the equipotential surfaces that are configured with respect to the antenna.

Taking into account the above, the method proposed in this work can be applied to any LEF measuring system that uses a parallel-plate antenna or another type of sensor (spherical antennas or vertical conductors). In addition, the antenna can be immersed in a space dominated by objects or structures that generate alterations on the electric field (buildings, metal towers, trees, mountains, etc.) and it can also be located at a certain height with respect to the ground plane. In general terms, the generalized process is composed of five stages (described below) and its scheme is shown in Fig. 2.

3.1. Stage 1 – Characterization of the Environment

In this stage it is necessary to collect a lot of information about the electromagnetic environment where the measuring system will be immersed. This information is related to the spatial distribution and shapes of the different structures and obstacles (trees, posts, metal structures, buildings, etc.) located in the vicinity of the antenna. Taking into account that all the elements that can affect the LEF measurement must be considered, a large enough area should be established. This area should have a radius that can vary from a few tens to several hundred meters from the measuring system.

Considering that tall buildings, close to the measuring system, shield or attenuate the electric fields produced by atmospheric discharges [21], [23], it is necessary to know both the height and the shape of the structures. With this information the results obtained by the simulation are optimal and close to reality. In this context, if there are no plans or detailed information on the area under study,

some tools that can facilitate this task are Google Maps®, Google Earth® and the Google Street View® application. These tools can provide updated and scaled information on the shape and height of the buildings that make up the physical environment to be simulated.

On the other hand, regarding to the structural characteristics of the buildings, some studies have concluded that the thickness of the walls and the metallic reinforcement produce slight changes in the electric field that is registered by the antenna (upper part of the buildings) [23]. For this reason, in simulations with a large number of elements it is recommended to model the structures as solid blocks that include the information of the materials that compose them (concrete, brick, wood, etc.). Likewise, for buildings composed of metal structures and glass facades, depending on the configuration, its framework can be modeled as a grounded Faraday cage.

It is important to highlight that the digital modeling of structures, buildings or objects can be streamlined using a 3D design software such as AutoCAD®, Inventor® or

SolidWorks®, among others. In this way, after digitizing the entire physical environment, the CAD file can be imported directly to the software where the electromagnetic simulations will be carried out. A couple of examples of this type of software are COMSOL Multiphysics® or CST Studio Suite®.

3.2. Stage 2 – Location and Type of Sensor

In order to define the location, it is recommended to install the sensor (parallel-plate antenna) in the highest structure available (environment modeled in stage 1). If this is not possible, the sensor must be installed as far away from the higher structures. This will prevent the attenuation of the electric field by neighboring structures and, consequently, the reduction in the magnitude of the recorded signatures [22]. In addition, it is important to keep in mind the physical height of the antenna, which will be given by the mast used for its installation.

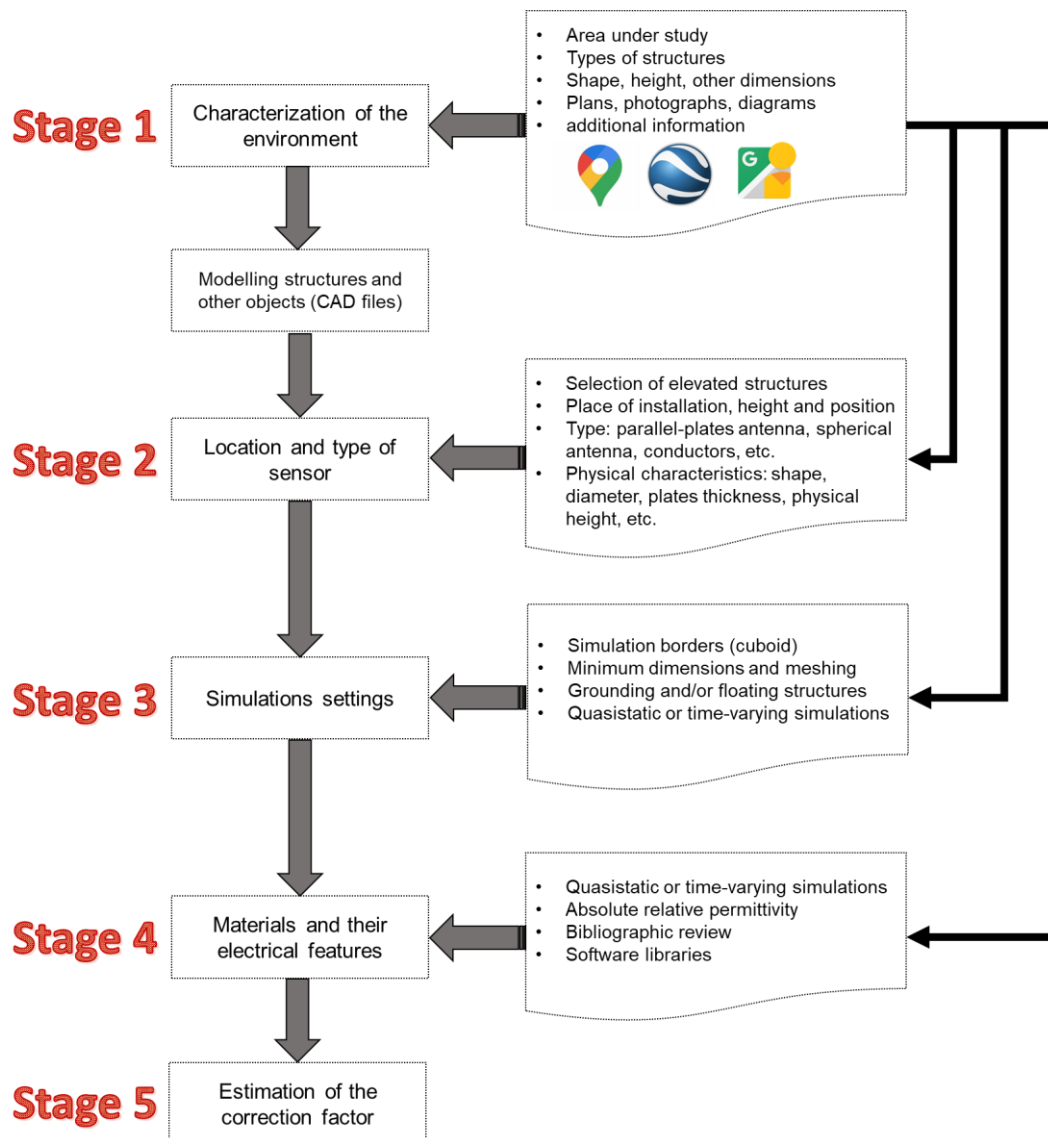


Fig. 2. Process to estimate the CFL for a lightning-generated electric field measuring system.

Regarding the shape of the sensor, the dimension (diameter) and the thickness of the aluminum plates must be considered. In the literature, some works can be found where these parameters have been analyzed [13], [21], [23]. Thus, Pinzón *et al.* shows in [23] that change in the LEF measurement due to variations in the shape of the upper plate of the antenna (Rogowski profile, semicircular or flat) is less than 3.6%. Moreover, after modifying the thickness of the sheets up to 25 times (from 2 mm to 50 mm), it was concluded that the changes in the LEF measurement are below 14%. These results show that these physical parameters can be considered of little relevance during antenna modeling.

Despite the above, other parameters such as the diameter of the plates and the insulation used for the separation between them can affect the capacitance of the antenna. Therefore, their influence on the measured electric field and the voltage difference that appears between the plates must be taken into account. This must also be considered when establishing the total correction factor of the measuring system, since the capacitance of the antenna, added to the capacitance of the short coaxial cable, affect the capacitive arrangement that is configured at the input of the electronic circuit [13], [25]. From these considerations, and maintaining similarity between LEF measuring systems, many studies use a 0.45 m diameter parallel-plate antenna with a separation of 0.03 m between them. For this configuration, using 3 mm thick aluminum sheets, the capacitance value of the antenna varies slightly between 59 pF and 62 pF [13], [25]–[27].

3.3. Stage 3 – Simulation Settings

Starting from the area defined for the antenna environment, it is necessary to establish the simulation settings. For this, it is recommended to include the structures, buildings, sensors and other elements in a test cube (cuboid) with a surface between three and five times greater than they occupy, and a height two or three times greater than the highest structure. After establishing the boundaries, in order to guarantee convergence in the simulation, it is necessary to establish a "zero-charge" condition in the bases of the structures, while the side faces and the underside of the cuboid are ground-referenced. Although this is generally a default condition in the simulator, it is important to verify the distances between the structures and the cuboid since insufficient space can affect the electric field behavior, and correspondingly, the voltage difference between the antenna plates.

In the same way, during simulations, it must be established if the structures are connected to the grounding system (through the structure itself or reinforcement) and they have a lightning protection system that provides electromagnetic shielding. If so, these structures must be referenced to ground in the simulations. Otherwise, it is recommended to leave the structures floating, a situation under which the results will

largely depend on the permittivity of the materials that make up the structures included in the tests.

Depending on the evaluation of the electric field, and the influence of the aspects mentioned in stages 1 and 2, to reduce the computation time it is desirable to carry out quasi-static simulations [23]. In addition, to reduce the complexity of the meshing, who plays a critical role in simulation speed and accuracy, and the amount of memory required, it is recommended use a time-domain or physics-controlled mesh (finite elements method). In any case, it is suggested to model the sensor with dimensions greater than 0.005% of the largest dimension of the cuboid defined as boundary. For example, for a cube with 400 meters on a side, the thickness of the sheets for a parallel-plate antenna must be at least 20 mm.

On the other hand, before including the sensor and structures, it is suggested to adjust the background electric field (initial conditions). To do this, a voltage can be defined on the upper face of the cuboid that, depending on its height, generates a vertical electric field whose magnitude is an integer value (1, 2, 5 or 10 V/m).

Finally, for the estimation of the vertical electric field using the simulator, two-dimensional vertical cuts that cross the antenna symmetrically can be handled. From this, the behavior of the electric field between the plates and the changes or deformations in the equipotential surfaces (perpendicular to the electric field) can be appreciated. To compute the electric field inside the antenna, two methods can be applied. First, using the voltage difference between the plates and their separation distance. The second one is based on the evaluation of the electric field at a specific point between the plates. For this method, it is recommended take the information at the central part of the antenna to avoid misinterpretation due to the increase of the electric field at the edges (edge effect).

3.4. Stage 4 – Materials and their Electrical Features

As mentioned in stage 1, it is important to know the electrical properties of materials since they can directly affect the behavior of the electric field. For this reason, it is convenient to identify the various materials that will be included during the simulations. Likewise, it is important to define if simulations will be performed in steady state or variable in time. In this context, [10] y [19] showed that that quasi-static simulations provide good results for this type of study without incurring high computational costs.

Considering that, under electrostatic conditions, the most important parameter in materials is the electrical permittivity, some references indicate that the relative permittivity of dry materials (without humidity) varies between 3 and 7 for those that have mineral components and from 2 to 5 for organic materials [28]. Likewise, simulation softwares have extensive libraries that include various materials whose electrical parameters are defined by default. However, it is recommended to use information from studies focused on the experimental characterization of materials used in civil construction.

Considering that wood and concrete are the most commonly materials used to simulate structures, several works affirm that the relative permittivity of wood changes according to frequency and it is influenced by factors such as the type of plant fiber, moisture, density and porosity [29], [30]. In the case of concrete and other building materials, the permittivity changes substantially in terms of frequency, humidity level and type of mixture [31]–[35].

Table 1 shows the relative permittivity of different materials that can be used in studies similar to the one

presented in this paper. From this summary, it is possible to observe that concrete is sensitive to its dry and liquid phases. In this way, a change in the water content of this dielectric causes its permittivity to be a complex variable that changes with the frequency of the electric field [33], [35]. For example, for dry concrete the relative permittivity can vary from 3 up to 9, but if concrete is wet the permittivity can take values between 5 and 18 for frequencies ranging from several hundred kHz to a few GHz. This frequency range can be related to the various events associated with the occurrence of a lightning flash.

Table 1. Apparent relative permittivity for various materials.

Material	Characteristics (Moisture content)	Frequency range	Apparent relative permittivity (ϵ_r) ⁺	Reference
Wood	Birch (12.5% - 15.5%)	5 kHz - 1 MHz	9 – 14	[29]
	Spruce (8.5% - 12%)	5 kHz - 1 MHz	6 – 12	[29]
	Fir (2% - 50%)	1 - 2 GHz	2 – 11	[30]
	Cherry (10% - 15%)	5 kHz - 1 MHz	8 – 11	[29]
	Dry cypress	50 Hz - 3 MHz	2 – 5	[36]
	Pine (9.5% - 15%)	5 kHz - 1 MHz	7 – 10	[29]
	Pine (2% - 50%)	1 - 2 GHz	2 – 14	[30]
	Oak (13.5% - 18%)	5 kHz - 1 MHz	13 – 18	[29]
	Fireproof plate *	5 - 100 MHz	4 – 9	[37]
	Anti-smoke plate *	5 - 100 MHz	3 – 8	[37]
	Medium density plate *	5 - 100 MHz	5 – 8	[37]
Brick	Dry	0.5 - 5 GHz	1.5 – 4	[38]
	Dry	5 GHz	4.2	[39]
	Dry	3 - 6 GHz	3.5	[40]
	Dry	2 - 6 GHz	4	[41]
	Dry	1 - 3 GHz	4.3	[42]
	Dry with holes	5 GHz	3.3	[39]
	Wet (2% - 11%)	3 - 6 GHz	5 – 15	[40]
Concrete	Dry (solid phase)	< 1 GHz	5 – 8	[32]
	Dry (solid phase)	250 - 700 MHz	6 – 7	[31], [35]
	Dry (solid phase)	< 5 GHz	3 – 7	[43]
	Dry (solid phase)	1 - 3 GHz	8 – 9	[42]
	Wet (14.5%)	250 - 700 MHz	8 – 18	[31], [35]
	Wet (up to 20%)	< 1 GHz	8 – 16	[32]
	Wet (1% - 15%) **	33 MHz	6 – 13	[33]
	Wet (1% - 15%) **	1 GHz	5 – 15	[33]
Clay/sand	Dry	< 1 GHz	4 – 8	[32]
	Wet	< 1 GHz	16 – 32	[32]
Stone	Dry	< 1 GHz	3 – 5	[32]
	Wet	< 1 GHz	5 – 26	[32]
Drywall	-----	1 - 3 GHz	2	[42]
Plexiglass	-----	4 - 6 GHz	2.5 – 3	[41]
Other materials	Asphalt	< 1 GHz	3 – 5	[32]
	Basalt	< 1 GHz	8	[32]
	Granite	< 1 GHz	5 – 7	[32]
Water	Temperature of 20 °C	1 GHz	80	[28]
	Temperature of 20 °C	10 GHz	64	[28]

⁺ The permittivity of some materials in presence of moisture is a complex amount $\epsilon_r = \epsilon_r' - j\epsilon_r''$;

* Composite wood materials; ** Steel reinforced

The values shown in this section for wood, concrete and other materials support the relevance of establishing the specific characteristics of all elements included in the simulation. In addition, although the information presented in Table 1 is a good starting point to select the permittivity of materials, it is recommended to review other data, especially that presented in Technical Note NIST 1536 [44].

3.5. Stage 5 - Estimation of the CFL

Considering that the purpose of the method proposed is to estimate the correction factor for any LEF measuring system, it is necessary to determine the electric field in the antenna under two conditions: (a) with the presence of structures and other objects (E_S); (b) without structures and other objects (E_{WO}). In this way, from simulations, and using equations (1) and (2), it is possible to compute the CFL which will indicate how many times the real electric field increases or decreases in the presence of the antenna and the structures around it.

$$E_{real} = \frac{E_{measured}}{CFL} \quad (1)$$

$$CFL = \frac{E_S}{E_{WO}} \quad (2)$$

4. Validation, Results and Discussion

After presenting the method, this section shows its validation process and the results obtained after its application. For this, the EMIR-UD measuring station, recently implemented by the GISE3 research group is used as a study case.

4.1. Characterization of the Physical Environment

The indirect lightning measuring station of the Universidad Distrital (EMIR-UD) is located south of Bogotá-Colombia (4.579° N, -74.158° W and 2550 meters above sea level) at the Faculty of Technology campus (FT-UD). In the initial stage, the parallel-plate antenna was installed on the roof of a three-story building at an approximate height of 13 meters. Under this consideration, the environment was delimited by an approximate area of 58000 m², which is equivalent to a circumference with a radius of 140 m. The area defined for this study (closed with the wide red line) is highlighted in Fig. 3.

The polygonal shape was defined to establish clear boundaries in the simulation and so that no structures were clipped. The area under study is characterized by being residential and partially commercial. The height of the structures varies between 5 and 16 meters, there are few trees and there are no complementary structures of higher height. The 3D environment, including the buildings inside the campus (brown central area in Fig. 3), residential complexes, houses and other structures, is shown in Fig. 4.



Fig. 3. Selected area for the study. Google Earth®

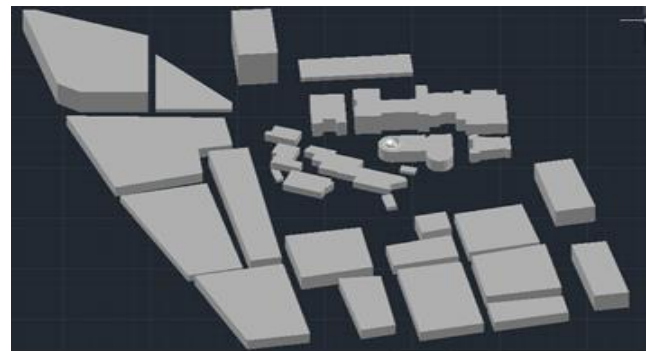


Fig. 4. 3D model implemented in AutoCAD®.

Once the area was defined, using the information provided by Google Maps®, all buildings and structures were modeled as blocks in three dimensions (3D) preserving their geometric shape. The software selected for this model was AutoCAD®. Likewise, based on the information taken from official plans of the university, the campus buildings were integrated into the environment with a higher level of detail.

4.2. Setup and Location of the Parallel-Plate Antenna

In this work, COMSOL Multiphysics® (finite element method) was selected for simulations. This decision was based on the following reasons: (a) it uses AutoCAD® files; (b) it has CAD tools for 3D modeling; (c) friendly graphical interface; (d) libraries with a large variety of materials; (e) meshes generated automatically or adaptively; and (f) the versatility to present results (2D cuts, 3D contours, potential distribution, magnitude and direction of the electric field, etc.). These characteristics make this software a versatile tool that can be used in a variety of studies in physics and engineering [45].

To reduce the computational costs, and due to the amount of memory available (8 GB), quasi-static field simulations using the AC/DC module were performed. In addition, a lightning discharge model was not included. This decision was based on the study presented by Pinzon *et al.* [23] where time-domain simulations using a double-exponential voltage pulse to the antenna were implemented. The comparison of results showed that maximum values and the enhance factor of the electric field in the sensor applying the varying-time pulse were the same as those obtained using a static voltage (corresponding to the pulse peak value).

On the other hand, the antenna was modeled as an arrangement of parallel-plates with separation of 0.03 m between them. The upper and lower plates have a circular shape with a diameter of 0.47 m and 0.45 m, respectively. Additionally, in order to reduce software requirements (meshing), the antenna was modeled using 0.03 m thick aluminum plates. This configuration was selected taking into account that the thickness variation of the plates does not significantly affect the electric field that appears in the antenna [23]. Based on these characteristics, Fig. 5 shows the antenna model, including a blue region between plates, which is associated with the dielectric material that separates them (generally air). In addition, a solid aluminum mast with 1.5 meters high and 0.06 m diameter was included.

During simulations, the antenna was located in two places: (a) case 1 - initial position: the roof of a three-story building in the FT-UD campus (Block 5) at a height of 13 meters; (b) case 2 - future position: roof of the new laboratories building (final height of 30 meters), whose completion is projected for 2022. These locations are shown in Fig. 6 and it can be seen that, even excluding the new building, currently Block 5 is not the tallest structure in the electromagnetic environment under study. This situation will have relevance in the results obtained with the simulator, which will be presented and analyzed later.

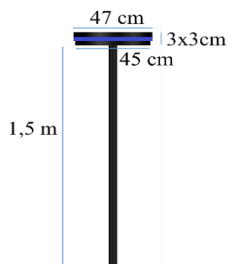


Fig. 5. Parallel-plate antenna, model implemented in COMSOL® including the mast.

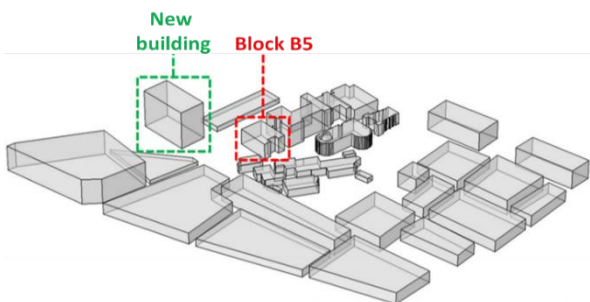


Fig. 6. Locations of the measuring system.

4.3. Simulation Settings

Once the 3D physical environment was implemented, COMSOL Multiphysics® software was used to define the simulation boundaries. For this, a cuboid 500 m long, 500 m wide and 100 m high was configured. In this way, the total simulation area (0.25 km²) is approximately four times the area containing the structures. An overview of the simulation environment implemented in COMSOL® is shown in Fig. 7 and Fig. 8. Furthermore, during simulations a physics-controlled mesh was used. This is a

simple and unstructured array, which is automatically created and adapted for the physical environment under study. The meshing sequence was based on free size tetrahedral structures. However, the element size was set to the following parameters: maximum size of 50 m; minimum size of 9 m; curvature factor of 0.5 m and resolution in narrow regions of 0.1 m.

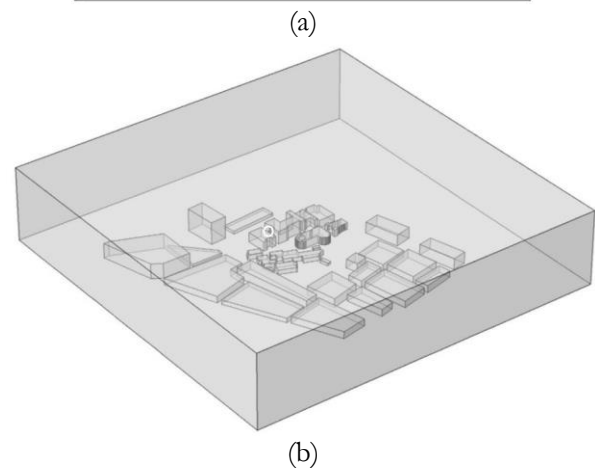


Fig. 7. Simulation environment implemented in COMSOL®. (a) top view; (b) 3D view.

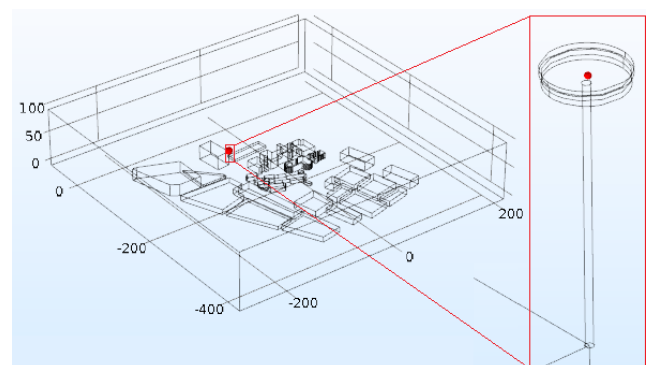


Fig. 8. Antenna installed on the roof of the new building (case 2) - 3D view.

On the other hand, the "zero charge" condition was established in the bases of the structures. In addition, the side faces and the base of the cuboid were ground-referenced, while a potential difference of 100 V was applied on the upper face. Using this configuration, a background vertical electric field of 1 V/m was established (without elements). Finally, taking into account that the thickness of the antenna was previously adjusted,

structures with dimensions less than 3 cm were not included and the automatic meshing defined by the simulator was used.

4.4. Selection and Adjustment Of Materials

For the study case, during the collection of information it was evidenced that in the vicinity of the university campus there are no metal structures or high-rise trees (less than 5 meters). From this condition, the materials defined to perform the simulations are as follows:

- The antenna (plates and mast) was made of Aluminum [99.5 & 0.24 mm grain size].
- The space around the structures and the antenna is air.
- Buildings, residential complexes, houses and other structures were modelled using concrete.

In order to estimate the electric field in the antenna as a function of the electrical properties of the concrete a set of tests was carried out. In this way, this parameter was modified from 5 to 15 in unit steps, all structures were included without connecting them to ground and the antenna was located in the two aforementioned places (Block 5 and new building). The results summarized in Table 2 show that, although permittivity increases three times in magnitude, the electric field decreases by 9% between extreme values for case 1 (Block 5) and increases by 15% for case 2 (new building). In fact, the reduction (attenuation) of the electric field in the first case is due to the shielding effect caused by the presence of the new building (30 meters) close to the antenna (13.5 meters).

Table 2. Electric field in the antenna (Block 5) as a function of the permittivity of the concrete.

Relative permittivity of concrete	Electric field (V/m)	
	Case 1 Block 5	Case 2 New building
5	1.088	2.746
6	1.084	2.817
7	1.077	2.877
8	1.068	2.929
9	1.057	2.974
10	1.047	3.017
11	1.034	3.053
12	1.023	3.086
13	1.012	3.117
14	1.001	3.143
15	0.989	3.167

From these tests it can be concluded that the relative permittivity of concrete can vary quite a bit without significantly affecting the electric field present in the antenna. Taking into account the above, for the remaining tests a permittivity of 8 will be established for this material. Finally, it is important to define whether the structures are grounded or floating. When the structures are grounded their influence on the electric field must be carefully evaluated, especially in objects of greater height. This is

because these structures can severely modify the vertical electric field and the equipotential surfaces arranged horizontally (perpendicular to the electric field). This effect will be evidenced in the results presented below.

4.5. Estimation of the CFL

The CFL indicates how many times the electric field is amplified or attenuated in the antenna due to its position and the surrounding environment. To evaluate this effect, several tests changing the location of the antenna and the connection of the structures to ground were carried out.

4.5.1. Cases with the floating antenna

At first, the antenna was left floating (ungrounded) and six scenarios were defined. The results for the electric field in the antenna are synthesized in Table 3, while the behavior of equipotential surfaces is shown in Fig. 9 (case 1) and Fig. 10 (case 2). These results were obtained using a cut in 2D (xz plane) on the symmetry axis of the antenna. For each scenario, the equipotential surfaces across the entire space are presented in the left column, while the voltage between the plates is shown in the right column using a different color map (scaled appropriately).

Starting with the initial condition without including structures (see Fig. 9(a)), the potential difference and the electric field between plates in the antenna were 43.5 mV and 1.452 V/m, respectively. These magnitudes are considered as the reference values and will be used to compare the results obtained with the other configurations. For the original location of the antenna in Block B5 (test 1-A), it is observed that the presence of floating structures (see Fig. 9(b)) attenuates the electric field by a factor of 0.862, while when using grounded structures (test 2-A, see Fig. 9(c)) the electric field decreases 0.647 times.

These results, excluding the new building, are due to the fact that Block 5 is not the tallest building in the original environment, which causes the electric field in the antenna to be attenuated by neighboring structures. Likewise, the effect of grounding structures is evident in Fig. 9(c), since the equipotential surfaces, especially those with a magnitude close to zero volts, are deformed by the presence of tall objects (approaching to the antenna). In this case, the voltage between the sensor plates and the electric field measured are reduced.

On the other hand, when the new building (NB) was included (tests 3-A and 4-A), the shielding effect caused by the presence of a structure twice as high (30 meters approx.) in the vicinity of the sensor is more evident (see Fig. 9(d) and Fig. 9(e)). Similar to reported in test 2-A, the grounded structures in test 4-A cause a decrease in the voltage that appears between the plates. Comparing with previous results, an additional attenuation of the electric field between 15% (test 1-A vs. test 3-A) and 5% (test 2-A vs. test 4-A) was observed. In these cases, including the new building, the CFL is 0.736 with the floating structures and 0.613 when they are grounded.

Table 3. Vertical electric field and CFL when the antenna is floating.

Test	Antenna location	Structures	Additional conditions	Voltage between plates (mV)	E with structures (V/m)	E without structures (V/m)	CFL
1-A	Block 5	Floating	without NB	37.5	1.251	1.452	0.862
2-A	Block 5	Grounded	without NB	28.2	0.939	1.452	0.647
3-A	Block 5	Floating	with NB	32.0	1.068	1.452	0.736
4-A	Block 5	Grounded	with NB	26.7	0.890	1.452	0.613
5-A	New building	Floating	-----	87.9	2.929	1.422	2.060
6-A	New building	Grounded	-----	185.1	6.170	1.422	4.339

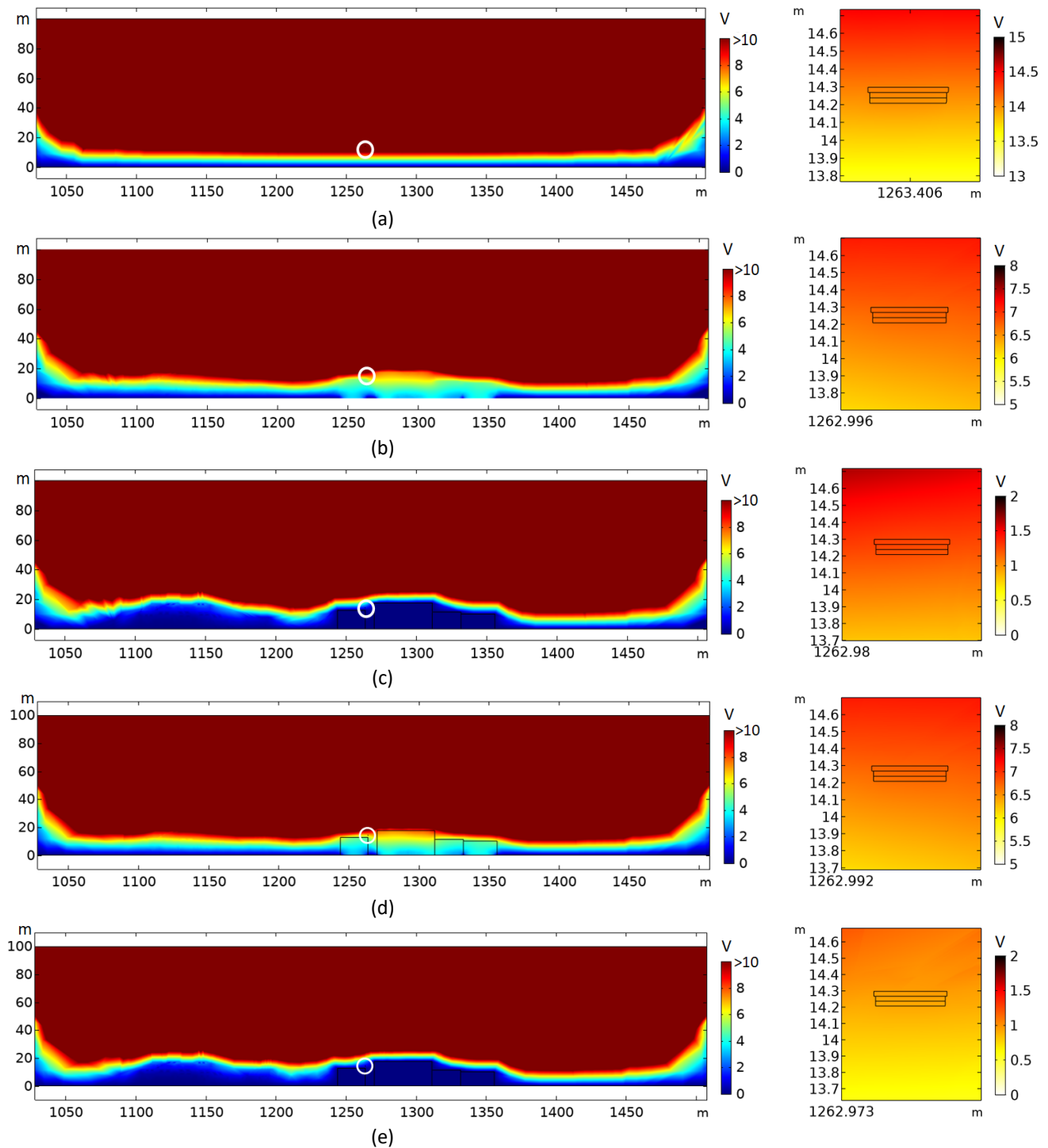


Fig. 9. Equipotential surfaces for case 1 (Block B5) when the antenna is floating (xz plane) (a) test without structures (reference); (b) test 1-A; (c) test 2-A; (d) test 3-A; (e) test 4-A.

Note: the white circle shows the position of the antenna – zoom in the left column.

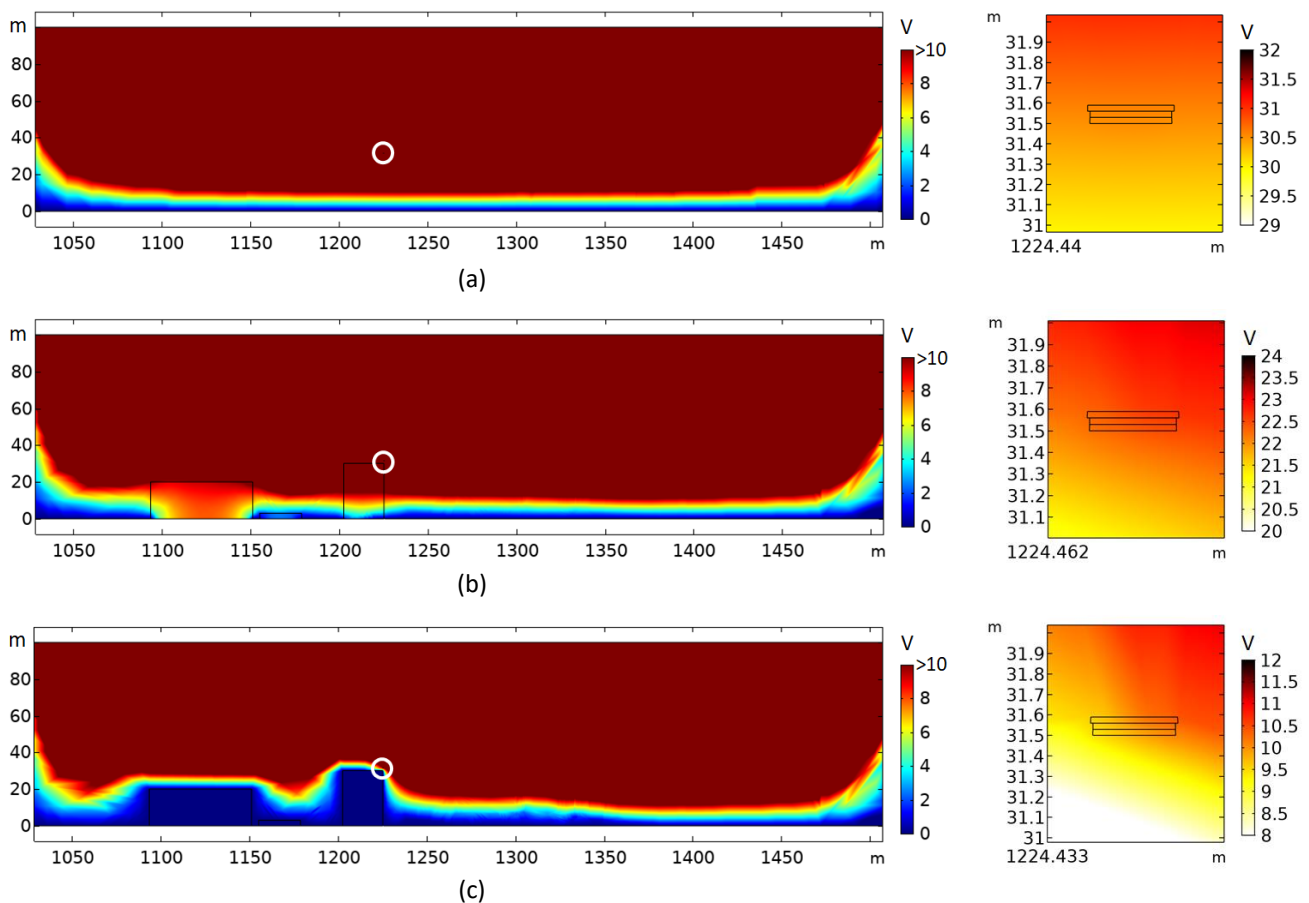


Fig. 10. Equipotential surfaces for case 2 (new building) when the antenna is floating (xz plane) (a) test without structures (reference); (b) test 5-A; (c) test 6-A.

Note: the white circle shows the position of the antenna – zoom in the left column.

In contrast, when the antenna is located at the top of the new building, and the structures are floating (test 5-A), the results show that the electric field increases 2.06 times. On the other hand, when all the structures are grounded the CFL is 4.34 (test 6-A). Furthermore, to illustrate the influence of the structures, Fig. 10(b) and Fig. 10(c) show the variation of the equipotential surfaces (seen as equipotential lines in 2D view) before and after grounding the structures, respectively.

These results are logical since the new building is the tallest structure in the simulated environment, there is no nearby shielding, and therefore, the electric field is intensified at the top of the building. Comparing test 5-A and test 6-A, it can be seen that the electric field increases more than two times when the structures are grounded. This is because floating structures do not significantly alter the trajectory of equipotential surfaces distributed perpendicular to the vertical component of the electric field (see Fig. 10(b)).

4.5.2. Cases with the antenna grounded

To complete the study, the effect when the bottom plate and the mast is connected to ground was evaluated. Table 4 shows the results for this condition. When the antenna is located in Block B5 (test 1 to 4) the reference value of the electric field is intensified 140 times (from

1.422 V/m up to 200.63 V/m). This is related to the increase of the voltage that appears in the antenna. In this condition, the bottom plate has 0 volts and the upper plate acquires the voltage of the equipotential surface which is located (6.02 V at 14.53 meters approximately). From these tests, it can be seen that the electric field is quite attenuated when the antenna is ground-referenced and is installed in a low-rise structure. Despite this condition, the CFL increases when the structures are floating (tests 1-B and 3-B). This effect is similar to that observed when the antenna was not connected to ground.

Regarding tests 5-B and 6-B (antenna located in the new building), the electric field increases from 1.55 up to 3.35 times depending on the configuration analyzed. The most critical condition can be seen in Fig. 11(b) when all elements are floating with exception of the antenna (test 5-B). In this case, the voltage between plates reaches 12.41 V and the electric field in the antenna is 413.61 V/m. These results are related to the phenomenon previously explained in which the elements connected to ground cause the low-magnitude equipotential surfaces to deviate and surround the structures and the antenna.

On the other hand, Fig. 12 complements the results obtained for test 6. First, when the antenna was floating in test 6-A (see Fig. 12(a)) the voltage between the plates was 0.185 V. Later, during test 6-B (see Fig. 12(b)), the zero-volt equipotential surface (dark blue) is initially located on

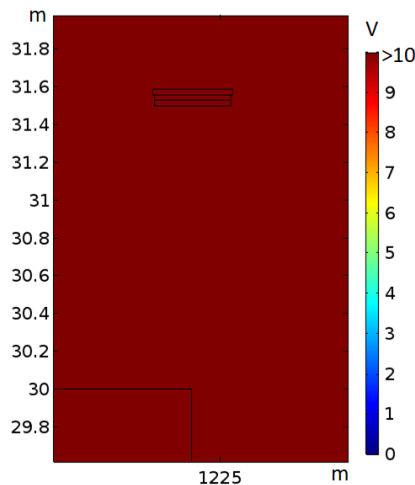
the structure and later it reaches the mast and the bottom plate of the antenna. For this case, the upper plate acquires a potential of 5.73 V. Under these conditions, the electric field in the sensor varies from 6.17 V/m (test 6-A) to 191.11V/m (test 6-B), although the latter is less severe than test 5-B where 413.61 V/m was obtained.

From simulations, it can be stated that the connection to ground of structures and/or the lower part of the antenna has effect on the equipotential surfaces less than 15 V, causing an increase in the electric field measured by the antenna. This behavior can be demonstrated in Fig. 12

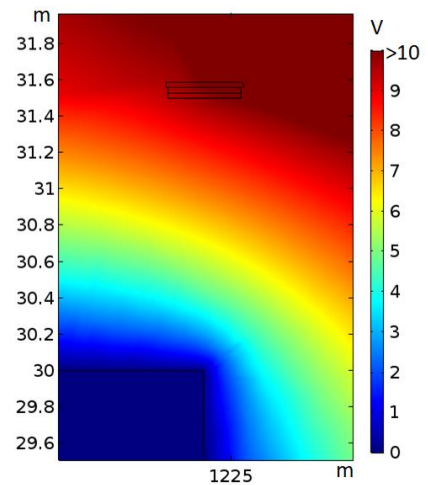
with the 6-Volts equipotential surface (yellow color). In this case, when the structures are grounded, the equipotential is located 31 meters high (above the structure), and once the new building ends, one meter away, the surface begins to decay crossing the elevation of 30.1 meters. On the other hand, when the structures and the antenna are connected to ground, the 6-Volts equipotential crosses over the building at approximately 31.2 meters, then, in the presence of the grounded antenna, ascends towards its upper plate (31.53 meters), and finally, when it separates from the antenna, the surface is located 30.6 meters high and continues to descend.

Table 4. Vertical electric field and CFL when the plate/mast of the antenna are grounded.

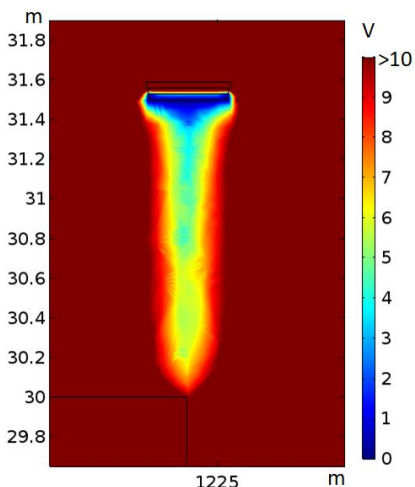
Test	Antenna location	Structures	Additional conditions	Voltage between plates (V)	E with structures (V/m)	E without structures (V/m)	CFL
1-B	Block 5	Floating	without NB	0.579	19.308	200.63	0.096
2-B	Block 5	Grounded	without NB	0.131	4.380	200.63	0.021
3-B	Block 5	Floating	with NB	2.044	68.140	200.63	0.339
4-B	Block 5	Grounded	with NB	0.338	11.269	200.63	0.056
5-B	New building	Floating	----	12.408	413.61	123.41	3.352
6-B	New building	Grounded	----	5.733	191.11	123.41	1.549



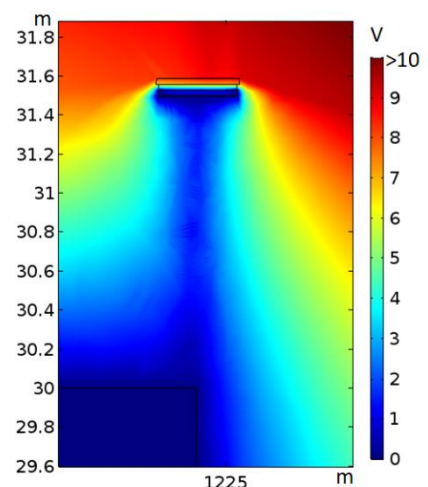
(a)



(a)



(b)



(b)

Fig. 11. Equipotential surfaces for test 5 with floating structures. (a) floating antenna (test 5-A); (b) bottom plate and mast grounded (test 5-B).

Fig. 12. Equipotential surfaces for test 6 with structures grounded. (a) floating antenna (test 6-A); (b) bottom plate and mast grounded (test 6-B).

In summary, the evidence presented in this section shows that LEF measurements carried out on low structures, even with those structures and/or the antenna grounded (mast and bottom plate), will always be attenuated or shielded by those objects of greater height that are located in the vicinity of the sensor (radius of influence between 10 and 30 meters). Thus, the best location for such a measuring system should be, as far as possible, the highest structure available in the physical environment.

Under this optimal location, grounding the lower part of the antenna, while ensuring the same reference for coaxial cables, circuit and recording equipment, can cause significant increases in both the electric field and the input voltage of the electronic circuit. This can cause buffer-amplifier saturation and changes in the LEF waveforms, especially those generated by nearby flashes (below 10 km). Likewise, under this configuration it is recommended to include a protection system against voltage surges, both for the electronics and for the recording equipment. However, regardless of the configuration analyzed, the process to determine the CFL will be framed in the method proposed and validated throughout this work.

5. Conclusions

In this paper, a practical method to evaluate the influence of nearby structures and other elements on the measurement of lightning-generated electric field (LEF) was presented. In this way, the influence of the shape of the antenna, its location, the physical environment, the relative permittivity of the structures and the effect of grounding various elements (buildings, lower plate of the antenna and mast) were analyzed. This method can be applied to any LEF measuring system that uses a parallel-plate antenna or another type of sensor, as long as its technical specifications (dimensions, materials, etc.) are available. In addition, the proposed process is more relevant if the antenna is located at a certain height with respect to the ground plane and it is immersed in a space dominated by elevated objects.

From simulations and an adequate modeling of the electromagnetic and physical environment, it was possible to demonstrate that the electrical permittivity of the concrete (material used for the structures) can alter the electric field up to 15%. Likewise, from the study case, it was confirmed that the signals acquired by the measuring system will always be affected by the presence of buildings. In this way, the installation of the sensor in low height places will be associated with the shielding produced by larger structures and the respective attenuation of the electric field. Otherwise, when the antenna is installed at a high point, the electric field is amplified.

On the other hand, the importance of establishing whether buildings are adequately connected to ground was demonstrated. The tests showed that grounded structures cause strong deflection (deformation) of equipotential surfaces, especially those of low magnitude (close to zero volts). This situation, added to the floating antenna

condition, causes a reduction in the potential difference that appears between the plates and a reduction in the measured electric field. Now, if it is decided connect to ground the antenna (bottom plate and mast) it must be taken into account that the potential difference in the antenna will be much greater and the intensity of the electric field will increase considerably. This condition can generate saturation in the electronic circuit, producing alterations in the recorded waveforms.

Based on previous works, in order to reduce complexity, simulation times and hardware requirements, the proposed method emphasizes the use of quasi-static conditions and the absolute permittivity of materials. However, the next stage of this research may be aimed at implementing full-wave simulations (3D full-wave) with large physical environments and evaluating the behavior of the horizontal component of the electric field.

Finally, it should be taken into account that the quantitative results presented in this work are only valid for the physical environment described in section 4. Also, it is important to remember that the CFL changes depending on the environment in which each measuring system is immersed and the installation place of the sensor. However, under any situation, it is enough to consider the suggestions and recommendations presented in section 3 and replicate the method proposed in this paper.

Acknowledgment

This work was developed by GISE3-UD research group with the financial support provided by CIDC – Universidad Distrital Francisco José de Caldas (research project with code 2-5-591-19)

References

- [1] V. Cooray, "The mechanism of the lightning flash," in *The Lightning Flash*. London: IEE Power Engineering Series, 2003, pp. 127–240.
- [2] S. R. Sharma, V. Cooray, M. Fernando, and F. J. Miranda, "Temporal features of different lightning events revealed from wavelet transform," *J. Atmos. Solar-Terrestrial Phys.*, vol. 73, no. 4, pp. 507–515, Mar. 2011. [Online]. Available: <http://www.sciencedirect.com/science/article/pii/S136468261000341X>
- [3] N. Azlinda Ahmad *et al.*, "The first electric field pulse of cloud and cloud-to-ground lightning discharges," *J. Atmos. Solar-Terrestrial Phys.*, vol. 72, no. 2–3, pp. 143–150, Feb. 2010, doi: 10.1016/j.jastp.2009.11.001.
- [4] N. A. Ahmad, Z. A. Baharudin, M. Fernando, and V. Cooray, "Radiation field spectra of long-duration cloud flashes," *Atmos. Sci. Lett.*, vol. 16, no. 2, pp. 91–95, 2015, doi: 10.1002/asl2.537.
- [5] C. Wooi, Z. Abdul-Malek, B. Salimi, N. A. Ahmad, K. Mehranzamir, and S. Vahabi-Mashak, "A comparative study on the positive lightning return stroke electric fields in different meteorological conditions," *Adv. Meteorol.*, vol. 2015, pp. 1–12, 2015,

- doi: 10.1155/2015/307424.
- [6] A. Nag, B. A. DeCarlo, and V. A. Rakov, "Analysis of microsecond- and submicrosecond-scale electric field pulses produced by cloud and ground lightning discharges," *Atmos. Res.*, vol. 91, no. 2–4, pp. 316–325, Feb. 2009, doi: 10.1016/j.atmosres.2008.01.014.
- [7] O. F. Escobar, H. E. Rojas, F. Román, and C. A. Cortes, "Lightning magnetic field measuring system in Bogotá — Colombia: Signal processing method," in *2013 International Symposium on Lightning Protection (XII SIPDA)*, 2013, no. 1, pp. 162–166.
- [8] O. F. Escobar, "Lightning magnetic field measuring system in Bogota, Colombia," Master thesis, Universidad Nacional de Colombia, 2013.
- [9] H. E. Rojas Cubides, "Técnicas avanzadas para el tratamiento y procesamiento de señales de campos electromagnéticos generados por rayos," (in Spanish) Ph.D. dissertation, Universidad Nacional de Colombia, 2018.
- [10] F. Santamaría, F. Vega, and F. Roman, "Calibration of a lightning electric field measuring system in Colombia," in *3rd Simposio Internacional sobre Calidad de la Energía Eléctrica SICEL*, 2005, pp. 1–5.
- [11] F. Santamaria, "Medición de campo eléctrico de rayos con una antena de placas paralelas en la ciudad de Bogotá y comparación con otras zonas del mundo," (in Spanish) Master thesis, Universidad Nacional de Colombia, Bogotá DC, Colombia, 2006.
- [12] H. E. Rojas, A. S. Cruz, and C. A. Cortés, "Characteristics of lightning-generated electric fields measured in the Bogotá Savanna, Colombia," *UIS Ing.*, vol. 16, no. 2, pp. 243–251, 2017. [Online]. Available: <http://revistas.uis.edu.co/index.php/revistausingenierias/article/view/6808>
- [13] H. E. Rojas, C. A. Rivera, J. Chaves, C. A. Cortés, F. J. Roman, and M. Fernando, "New circuit for the measurement of lightning generated electric fields," in *2017 International Symposium on Lightning Protection (XIV SIPDA)*, 2017, pp. 1–7.
- [14] M. I. Nino, H. E. Rojas, and F. Roman, "Characterization of positive return strokes from a thunderstorm day observed in Bogota, Colombia," in *2019 International Symposium on Lightning Protection (XV SIPDA)*, Sep. 2019, pp. 1–6, doi: 10.1109/SIPDA47030.2019.8951668.
- [15] C. A. Granados, H. E. Rojas, and F. J. Román, "Features of the initial breakdown pulses in negative ground flashes observed in Colombia," in *2019 International Symposium on Lightning Protection (XV SIPDA)*, 2019, pp. 1–6.
- [16] C. A. Granados, H. E. Rojas, C. A. Rivera, and F. J. Román, "Characterization of electric fields produced by preliminary breakdown pulses observed in Bogotá, Colombia," in *Lecture Notes in Electrical Engineering*. Springer, Cham, 2020, pp. 1235–1243.
- [17] S. Bonyadi-Ram, R. Moini, S. H. H. Sadeghi, and A. Mahanfar, "The effects of tall buildings on the measurement of electromagnetic fields due to lightning return strokes," *IEEE Int. Symp. Electromagn. Compat.*, vol. 2, pp. 1001–1004, 2001, doi: 10.1109/ISEMC.2001.950533.
- [18] F. Rachidi, W. Janischewskyj, A. M. Hussein, C. A. Nucci, S. Guerrieri, and B. Kordi, "Current and electromagnetic field associated with lightning-return strokes to tall towers," *IEEE Trans. Electromagn. Compat.*, vol. 43, no. 3, pp. 356–367, 2001, doi: 10.1109/15.942607.
- [19] Y. Baba and V. A. Rakov, "Lightning electromagnetic environment in the presence of a tall grounded strike object," *J. Geophys. Res.*, vol. 110, no. D9, p. D09108, 2005, doi: 10.1029/2004JD005505.
- [20] Y. Baba and V. A. Rakov, "Electromagnetic fields at the top of a tall building associated with nearby lightning return strokes," *IEEE Trans. Electromagn. Compat.*, vol. 49, no. 3, pp. 632–643, 2007, doi: 10.1109/TEMC.2007.902402.
- [21] A. Mosaddeghi, D. Pavanello, F. Rachidi, M. Rubinstein, and P. Zwiackier, "Distortion of electric and magnetic fields from lightning due to close-by metallic structures," in *7th International Symposium on Electromagnetic Compatibility and Electromagnetic Ecology*, Jun. 2007, pp. 249–253, doi: 10.1109/EMCECO.2007.4371702.
- [22] A. Mosaddeghi, D. Pavanello, F. Rachidi, M. Rubinstein, and P. Zwiackier, "Effect of nearby buildings on electromagnetic fields from lightning," *J. Light. Res.*, vol. 1, no. 1, pp. 52–60, 2009, doi: 10.2174/1652803400901010052.
- [23] A. L. Pinzon, H. E. Rojas, and F. J. Roman, "Influence of the antenna and the neighboring structures in the measurement of lightning-generated electric fields," in *2019 IEEE 39th Central America and Panama Convention (CONCAPAN XXXIX)*, Nov. 2019, pp. 1–6, doi: 10.1109/CONCAPANXXXIX47272.2019.8976938.
- [24] D. E. Crawford, "Multiple-station measurements of triggered lightning electric and magnetic fields," Master thesis, University of Florida, 1998.
- [25] A. Galvan and M. Fernando, *Operative Characteristics of a Parallel-plate Antenna to Measure Vertical Electric Fields from Lightning Flashes*, 1st ed. Uppsala, Sweden: Uppsala University, 2000.
- [26] V. Cooray and S. Lundquist, "Characteristics of the radiation fields from lightning in Sri Lanka in the tropics," *J. Geophys. Res.*, vol. 90, no. D4, p. 6099, 1985, doi: 10.1029/JD090iD04p06099.
- [27] Z. A. Baharudin, N. A. Ahmad, J. S. Mäkelä, M. Fernando, and V. Cooray, "Negative cloud-to-ground lightning flashes in Malaysia," *J. Atmos. Solar-Terrestrial Phys.*, vol. 108, pp. 61–67, 2014, doi: 10.1016/j.jastp.2013.12.001.
- [28] Z. Hlavacova, "Electrical properties of some building materials," in *Research and Teaching of Physics in the Context of University Education*, 2007, no. 2005, pp. 134–140.
- [29] K. Pento, T. Wysocza, L. Sciences, L. Sciences, A. E. Wroc, and R. January, "Dielectric properties of

- selected wood species in Poland,” *Wood Res.*, vol. 62, no. 5, pp. 727–736, 2017, [Online]. Available: <http://www.woodresearch.sk/wr/201705/06.pdf>
- [30] S. Razafindratsima, Z. M. Sbartai, and F. Demontoux, “Permittivity measurement of wood material over a wide range of moisture content,” *Wood Sci. Technol.*, vol. 51, no. 6, pp. 1421–1431, 2017, doi: 10.1007/s00226-017-0935-4.
- [31] K. Pokkuluri, “Effect of admixtures, chlorides, and moisture on dielectric properties of Portland cement concrete in the low microwave frequency range,” Master's Thesis, Virginia Polytechnic Institute and State University, Blacksburg, VA, 1998.
- [32] K. Meyer, E. Erdogmus, G. Morcou, and M. Naughtin, “Use of ground penetrating radar for accurate concrete thickness measurements,” in *Proceedings of the AEI 2008 Conference - AEI 2008: Building Integration Solutions*, 2008, vol. 328, no. September, pp. 1–10, doi: 10.1061/41002(328)67.
- [33] M. Fares, Y. Fargier, G. Villain, X. Derobert, and S. P. Lopes, “Determining the permittivity profile inside reinforced concrete using capacitive probes,” *NDT E Int.*, vol. 79, pp. 150–161, 2016, doi: 10.1016/j.ndteint.2016.01.002.
- [34] J. Hu, A. Alzeyadi, Q. Tang, and T. Yu, “Characterization of dielectric constant of masonry wall using synthetic aperture radar imaging,” in *SPIE Smart Structures + Nondestructive Evaluation*, 2019, no. April, p. 27, doi: 10.1117/12.2514068.
- [35] C. A. Granados, H. E. Rojas, and F. Santamaria, “Evaluación del apantallamiento electromagnético del concreto a partir de simulaciones en alta frecuencia y la aplicación del modelo de Jonscher,” *Ingeniería*, vol. 25, no. 2, pp. 1–15, 2020, doi: <https://doi.org/10.14483/23448393.15611> (in Spanish).
- [36] M. Norimoto, “Dielectric properties of wood,” *Bull. Wood Res. Inst. Kyoto Univ. Res. Inst. Kyoto Univ.*, vol. 59/60, pp. 106–152, 1976.
- [37] K. C. Varada Rajulu and B. N. Mohanty, “Dielectric and Conductivity Properties of Some Wood Composites,” *Int. J. Eng. Technol.*, vol. 8, pp. 51–60, 2016, doi: 10.18052/www.scipress.com/ijet.8.51.
- [38] B. Kapilevich and B. Litvak, “Microwave Characterization of Composite Building Materials,” in *Twelfth Israeli-Russian Bi-National Workshop 2013*, 2013, pp. 251–258.
- [39] Y. Pinhasi, A. Yahalom, and S. Petnev, “Propagation of ultra wide-band signals in lossy dispersive media,” in *2008 IEEE International Conference on Microwaves, Communications, Antennas and Electronic Systems, COMCAS 2008*, 2008, no. June, pp. 1–10, doi: 10.1109/COMCAS.2008.4562803.
- [40] P. D’Atanasio, A. Zambotti, S. Pisa, E. Pittella, and E. PiuZZi, “Complex permittivity measurements for moisture and salinity characterization of building materials,” in *IMEKO International Conference on Metrology for Archaeology and Cultural Heritage, Metro.Archeo 2017*, 2019, pp. 437–441.
- [41] S. Pisa, E. Pittella, E. PiuZZi, P. D’Atanasio, and A. Zambotti, “Permittivity measurement on construction materials through free space method,” in *2017 IEEE International Instrumentation and Measurement Technology Conference (I2MTC)*, 2017, pp. 8–11, doi: 10.1109/I2MTC.2017.7969867.
- [42] C. Thajudeen, A. Hoorfar, and F. Ahmad, “Measured complex permittivity of walls with different hydration levels and the effect on power estimation of TWRI target returns,” *Prog. Electromagn. Res. B*, vol. 30, no. May, pp. 177–199, 2011, doi: 10.2528/PIERB10091004.
- [43] D. McGraw, “The measured of the dielectric constant of three different shapes of concrete blocks,” *Int. J. Recent Res. Appl. Stud.*, vol. 25, no. 3, pp. 82–102, 2015, [Online]. Available: http://www.arpapress.com/Volumes/Vol25Issue3/IJRRAS_25_3_05.pdf.
- [44] J. Beker-Jarvis *et al.*, *NIST Technical Note 1536: Measuring the Permittivity and Permeability of Lossy Materials: Solids, Liquids, Metals, Building Material, and Negative-Index Materials*. USA, 2005, p. 150.
- [45] J. Ma and C. Koutsougeras, “Effects of design parameters on the fluid flow and the efficiency of single ended evacuated tubular solar thermal collectors via fem modelling and experimentation,” *Eng. J.*, vol. 19, no. 5, pp. 69–80, 2015, doi: 10.4186/ej.2015.19.5.69.



Albeiro Santa-Acosta, received the BSc. degree (5-years with honors) in Electrical Engineering from Universidad Distrital Francisco José de Caldas, Bogotá, Colombia in 2021. From 2018 to 2021, he was undergraduate researcher at the Electrical Systems and Energy Efficiency research group (GISE3-UD). Since 2020, he is with Ingenieros Emetres SLP (IM3) as auxiliary engineer. His research interests include lightning measurements, signal processing, design and planning of distribution and transmission systems.



Lina María Morales-García, received the BSc. degree (5-years with honors) in Electrical Engineering from Universidad Distrital Francisco José de Caldas, Bogotá, Colombia in 2021. From 2018 to 2021, she was undergraduate researcher at the Electrical Systems and Energy Efficiency research group (GISE3-UD). Since 2020, she is with WSP South America as junior engineer. Her research interests include lightning measurements, power quality disturbances, design and management of electrical and energy projects.



Herbert Enrique Rojas-Cubides was born in Bogotá DC, Colombia. He received the BSc. (5-years with honors), the M.Sc. degree in High Voltage and the Ph.D. degree in Electrical Engineering from Universidad Nacional de Colombia in 2003, 2007 and 2018, respectively. From 2010 to 2012 he received a full Doctoral Scholarship and he was researcher with the Electromagnetic Compatibility research group (EMC-UNC) at the same institution. In 2016, he was a visiting doctoral student at Atmospheric and Lightning Physics research group in University of Colombo, Sri Lanka. During 2017, he was a visiting researcher at Institute of Energy Systems, Energy Efficiency and Energy Economics (IE3) in Technical University of Dortmund, Germany. Since 2012, he has been with the Electrical Engineering Department (Faculty of Engineering) of the Universidad Distrital

Francisco José de Caldas where currently he is a Full Professor and Head-Researcher at Electrical Systems and Energy Efficiency research group (GISE3-UD). His research interests include high voltage and grounding technology, signal processing, lightning characterization, lightning detection, electromagnetic compatibility, power quality and energy demand.